Original Article

Evaluation of Mean Glandular Dose and Modulation Transfer Function for Different Tube Potentials and Target-Filter Combinations in Computed Radiography Mammography

Siti Aishah Abdul Aziz, Abdul Khaliq Mohd Saparudin, Ahmad Zaky Harun

Submitted: 30 Oct 2012
Accepted: 1 Apr 2013

Medical Radiation Programme, School of Health Sciences, Universiti Sains Malaysia, Health Campus, 16150 Kubang Kerian, Kelantan, Malaysia

Abstract

Background: **Different target-filter combinations in computed radiography have different impacts on the dose and image quality in digital radiography. This study aims to evaluate the mean glandular dose (MGD) and modulation transfer function (MTF) of various target-filter combinations by investigating the signal intensities of X-ray beams.**

Methods: **General Electric (GE) Senographe DMR Plus mammography unit was used for MGD and MTF evaluation. The measured MGD was compared with the dose reference level (DRL), whereas the MTF was evaluated using ImageJ 1.460 software. A modified Mammography Accreditation Phantom RMI 156 was exposed using different target-filter combinations of molybdenum-molybdenum (Mo-Mo), molybdenum-rhodium (Mo-Rh) and rhodium-rhodium (Rh-Rh) at two different tube voltages, 26 kV and 32 kV with 50 mAs.**

Results: **In the MGD evaluations, all target-filters gave an MGD value of < 1.5 mGy. The one-way ANOVA test showed a highly significant interaction between the MGD and the kilovoltage and target-filter material used (26 kV: F (2,12) = 49,234, *P* = 0.001;32 kV: F (2,12) = 89,972, *P* = 0.001). A Tukey post-hoc test revealed that the MGD for 26 kV and 32 kV was highly affected by the target-filter combinations. The test of homogeneity of variances indicates that the MGD varies significantly for 26 kV and 32 kV images (0.045 and 0.030 (*P* < 0.05), respectively). However, the one-way ANOVA for the MTF shows that no significant difference exists between the target-filter combinations used with 26 kV and 32 kV images either in parallel or perpendicular to the chest wall side F (2,189) = 0.26, *P* > 0.05).**

Conclusions: **Higher tube voltage and atomic number target-filter yield higher MGD values. However, the MTF is independent of the X-ray energy and the type of target-filter combinations used.**

Keywords: *mean glandular dose (MGD), modulation transfer function (MTF), computed radiography, spatial resolution, image processing*

Introduction

The medical society has expressed serious concern regarding the carcinogenic risk associated with the absorbed dose to the glandular tissue of the breast (1). The mean glandular dose (MGD) is defined as the average radiation absorbed dose to the breast glandular tissue in mammography examinations. The MGD estimation includes the measurements of incident air kerma, correction factors related to the backscatter factor, air kerma to glandular dose conversion, breast glandularity, and the X-ray spectrum. Molybdenum (Mo), rhodium (Rh) and tungsten (W) are the three elements used in mammography X-ray tubes to produce the optimal energy required (2). Meanwhile, filtration is used to remove the low- and high-energy X-rays in the bremsstrahlung spectrum (3).

The spectral quality of X-ray beams strongly influences diagnostic quality, such as the modulation transfer function (MTF), as a function of the object size. However, high X-ray spectral quality produced by higher kV and high atomic number target-filter combinations yield higher MGD. Ranger et al. (4), investigated the low-contrast breast masses in digital mammography. They used a breast-equivalent phantom in various configurations and concluded that the contrast-to-noise ratio (CNR) is strongly correlated to exposure and dose through the normalisation of relative signal-difference-to-noise-ratio (sdNR)

with the MGD. Glandular dose can be estimated by using a known incident exposure dose, spectral characteristics (target-filter, kVp and half-value layer (HVL)) and relevant breast phantom characteristics (thickness and glandular fraction) (4).

This study aimed to characterize the MGD and MTF values of different tube potentials and target-filter combinations in computed radiography (CR) mammography for optimizing clinical outcomes. Considering the importance of differences among the signal intensity measurements of object materials in breasts, this study was performed to relate the beam spectral with the image quality produced for dose-saving purposes. The first objective of this study was to determine the MGD values for 26 kV and 32 kV tube potentials with different target-filter combinations. MGD values are expected to increase with increased X-ray energy spectra and higher atomic number filter. The MGD values will be tested by one-way analysis of variation (ANOVA) to determine the significant MGD interactions with different tube potentials and target-filter combinations. The second objective was to evaluate the spatial resolution of the CR mammography using the same set of tube potentials and target-filter combinations as mentioned earlier in the parallel and perpendicular orientations to the chest wall. The MTF will be obtained using ImageJ 1.460 software, and the result will be evaluated using one-way ANOVA in terms of relating the spatial resolution with different tube potentials and target-filter combinations.

Medical image quality assessment is based on several principal components, including contrast, noise and spatial resolution; however, system performance is determined on the basis of spatial resolution. Spatial resolution refers to the smallest object sizes that can be distinguished by an imaging system. The Point Spread Function (PSF), which describes the response of an imaging system to a point stimulus, provides a more detailed description of the system's spatial resolution properties. Another spread function is the Line Spread Function (LSF), which refers to the linear stimulus responses and can be considered a linear collection of numerous PSFs. LSF is measured by using a slit image where the 90° profile across the slit is considered (5).

Besides spatial resolution, imaging system performance can also be determined by the manner in which the inherent contrast of an imaged object is lost in the imaging system as spatial frequency increases. Once the LSF is measured, the MTF can be computed directly from the LSF by using Fourier Transformation (FT) (6). A resolution test pattern, which is the line pair test pattern or star pattern, is used to measure the MTF. This method is not as accurate as the LSF method; however, it is sufficient to evaluate the sinusoidal signal intensity of X-ray beams. Therefore, the input to the output signal ratio can be measured to obtain the MTF values for each frequency tested.

Materials and Methods

Materials

This study was conducted using the General Electric (GE) Senographe DMR Plus mammography unit (Tube Model No.: Z.1B2B1.4A52) in the Radiology Department, Hospital Universiti Sains Malaysia. The X-ray tube contains molybdenum and rhodium anode material and inherent filtration of 0.8 mm beryllium. However, additional filtration options are also available. The optional filters are 0.03 mm thick molybdenum, 0.025 mm thick rhodium and 1.0 mm thick aluminium. The mammography unit can provide X-ray beams in the range of 22 kVp to 49 kVp at 4–600 mAs. A moving-type grid is installed with two focal spot sizes: 0.1 mm for small and 0.3 mm for large field sizes. The field sizes are 9 × 9 cm^2, 18 × 24 cm^2 and 24 × 30 cm^2 (7).

PTW Unidos E was used to measure dose, dose rate, dose length product, charge, and current. The dosimeter collects the cumulated charge in the unit of nanoCoulomb (nC). The dosimeter was calibrated using the air kerma method for specific beam quality related to the target-filter combination to pertain to the detector calibration factor, Nk (Gy/C). This dosimeter was paired with Shadow Free Diagnostic (SFD) ionization chambers type 30 469 for mammography (8). For mammography setting, the dosimeter was set to operate at 200 V with positive polarity. It had a sensitive volume of 6 cm^3 for mammography beam qualities in the range of 25 kV to 35 kV, which was specified by the manufacturer to be less than or equal to ± 2% (8).

For the measurement of entrance surface air kerma, the Mammography Accreditation Phantom RMI 156 was used. It attenuates X-ray beams in the same manner as that in the human breast and comprises 50% adipose tissue and 50% glandular tissue compressed to a thickness of 4.5 cm, which is equivalent to a 5.3 cm thick breast. The phantom is made of acrylic (9); its dimensions are 10.2 × 10.8 × 4.5 cm and weighs 0.91 kg. The original model of this accreditation phantom contains a wax block, which comprises

several test objects for conducting image quality assessments. We needed a modified phantom to provide information in terms of MTF and dose reduction factors for different target-filter. Because the standard RMI 156 did not have the pattern for spatial resolution evaluation, the wax insert was removed and substituted with an acrylic block of approximately the same dimensions and two sheets of resolution test pattern were placed in horizontal and vertical directions at the centre of the phantom, as shown in Figure 1. The same material from the RMI 156 and the acrylic block insert provided a uniform backscatter during irradiation. The pattern and orientation of this modified phantom was similar to that of the CIRS 11A phantom (10).

The Resolution Test Pattern (Model No.: 07-555) by Fluke Biomedical was actually an accessory for the Contrast and Resolution Mammography Phantom. Gold-nickel construction, equivalent to 25 microns of lead and 2.6 mm of aluminium, was used to design the line pair pattern. This construction was 25 mm long and 12.5 mm wide. The thickness of the line pair was 0.0175 mm, the sum of 0.0152 mm gold, and 0.0025 mm nickel. The number of line pairs ranged from 5 to 20 line pairs per mm (lp/mm) (11).

For the evaluation of X-ray beam intensities across the resolution test pattern image, the ImageJ 1.46o software was used. This freeware image processing and analysing program is capable of displaying, editing, analysing, processing, saving and printing in 8-bit, 16-bit, and 32-bit. ImageJ software is designed to read various types of image formats, including DICOM, TIFF, JPEG, GIF, BMP, etc. It can calculate the area and pixel value, measure distances and angles, and create density histograms and line profile plots for user-defined selections. Besides other options, users can zoom the image in or out up to 32 times their original display (12).

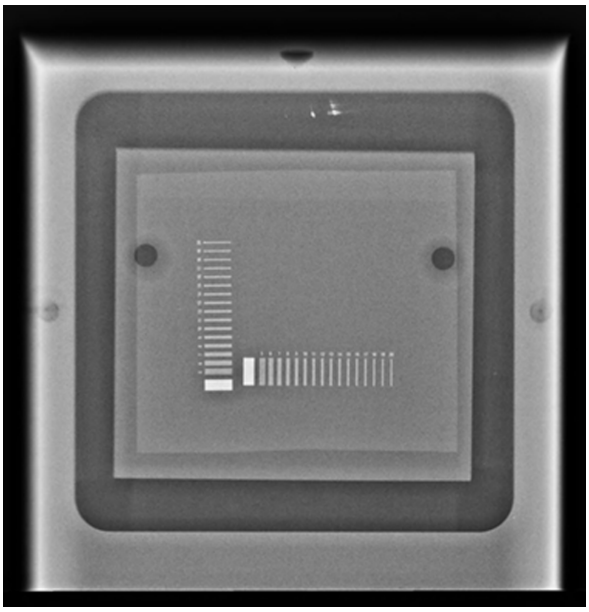

Figure 1: Resolution test pattern placed in horizontal and vertical direction at the center of the modified RMI 156 mammography phantom.

Determination of MGD

The MGD was determined by measuring the entrance surface air kerma, considering several correction factors proposed by Dance et al. (13), as follows:

$$MGD = K \,.\, g.\, c.\, s \qquad (1)$$

where K refers to the entrance air kerma at a point surface of the phantom measured without backscatter, g is the incident air kerma to mean glandular dose conversion factor in 50% glandularity (g-factor) for a range of half-value layers (HVLs) and breast thicknesses, c is the correction factor for any difference in 50% glandularity breast composition for women in the age group of 40–64 years and is the correction factor for any difference from the type of X-ray spectrum based on target-filter combinations.

The tube output in terms of the entrance surface air kerma per mAs was measured using the PTW Unidose E dosimeter and SFD ionization chamber. This was performed on the Mammography Accreditation Phantom RMI 156 placed in parallel to the compression paddle (craniocaudal view (CC) of mammography). The measured entrance surface air kerma was expressed in terms of nC, recorded from the dosimeter. These values were converted to mili-Grey (mGy) by using the detector calibration coefficient, N_k (Gy/C). This coefficient was obtained from the calibration certificate based on the specific beam quality, which was related to the target-filter combination. The SFD ionization chamber was placed above the compression paddle, with its focus side facing the source. The chamber was positioned at the centre of the field and 4 cm away from the chest wall edge, and it was connected to the dosimeter by a cable. The field size was set to 13 × 18 cm, which was larger

than the size of the phantom, to allow for adequate backscatter radiation, as shown in Figure 2 (a).

Initial exposures of the upper and lower limits for usual mammographic tube voltage were recorded (26 kV and 32 kV). The tube current-time product was set to be constant at 50 mAs for the tube voltages stated above with a focal-to-chamber distance of 60.5 cm. Subsequently, exposure was repeated five times with different anode target-filter combinations. Three choices of target-filter combinations were tested for this study: molybdenum-molybdenum (Mo-Mo), molybdenum-rhodium (Mo-Rh) and rhodium-rhodium (Rh-Rh) combinations. The resulting doses from different target-filter combinations and tube voltages were compared with the European Standard Diagnostic Reference Level (DRL) (14).

Determination of spatial resolution for MTF curve measurement

The images of the line pair patterns for the parallel and perpendicular orientations to the chest wall side were obtained by setting up the accreditation phantom and the mammography unit, as shown in Figure 2 (b). The exposures were conducted with the same exposure parameters as those used in the MGD measurement procedure. Subsequently, the exposed CR cassettes were processed using Kodak DirectView CR850 to obtain the digital images without any adjustments or enhancements. Following this, the digital images were exported into Digital Imaging and Communications in Medicine (DICOM) format to retain the raw data of the images.

Evaluation of MTF curve for image quality determination

The DICOM 16-bit images were imported into the ImageJ software for enabling readability and analysis. First, the images were converted into 8-bit images. In an 8-bit image, the colour index is expressed on a scale of 0 to 255, where 0 and 225 represents white and black, respectively. The image was zoomed to 100% to visualize all the line pair patterns. A straight line was drawn at the centre of the line pair patterns and the grey value of each of the pixels in that line was measured. These grey values were plotted on a graph to obtain a multiple sinusoidal signal. This multiple sinusoidal signal represents each group of the line pair per mm in a line pair test pattern.

The maximum and minimum intensities were identified and the ratio of the difference between the maximum (I_{max}) and minimum (I_{min}) signal intensities to the sum of both these signal intensities was determined by using the following modulation equation (*MTF*) by Bourne (5):

$$MTF = \frac{I_{max}-I_{min}}{I_{max}+I_{min}} \qquad (2)$$

The signal intensities were displayed in the form of sinusoidal intensity change. The MTF curves for a line pair test pattern were plotted with the MTF on the y-axis and the frequency of the line pair pattern was plotted on the x-axis.

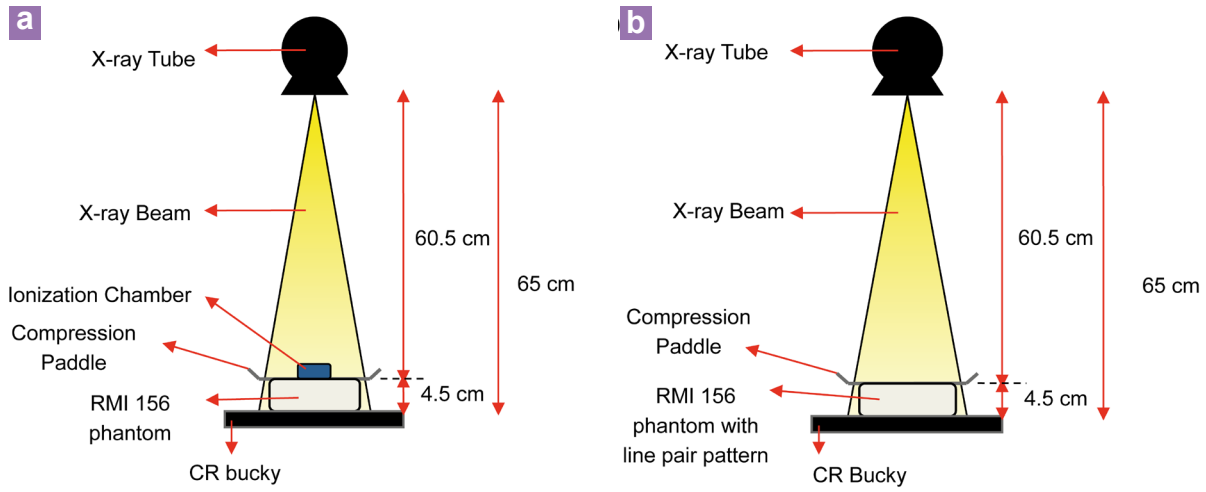

Figure 2: Equipment setup for (a) mean glandular dose measurement and (b) modulation transfer function measurement.

Results

Evaluations of MGD for different target-filter combinations

Table 1 shows the MGD measurements for different target-filter materials. The results specified that the absorbed dose for glandular breast tissue was lower for low voltage exposure, which used 26 kV in the mammography procedure, compared to that for high voltage exposure, which used 32 kV. The one-way ANOVA test was conducted to evaluate the impact of different target-filter combinations on MGD. The test of homogeneity of variances shows that the MGD varies significantly for 26 kV and 32 kV images (0.045 and 0.030 ($P < 0.05$), respectively). A Tukey post-hoc test revealed that the MGD for 26 kV using Mo-Mo = 0.68 + 0.001 mGy, $P = 0.001$; Mo-Rh = 0.57 + 0.001 mGy, $P = 0.001$ and Rh-Rh = 0.74 + 0.001 mGy, $P = 0.001$. The MGD for 32 kV using Mo-Mo = 1.44 + 0.001 mGy, $P = 0.001$; Mo-Rh = 1.24 + 0.001 mGy, $P = 0.001$ and Rh-Rh = 1.51 + 0.001 mGy, $P = 0.001$. The results also show a significant interaction between different tube potentials and target-filter material used (26 kV: $F(2,12) = 49{,}234$, $P < 0.05$; 32 kV: $F(2,12) = 89{,}972$, $P < 0.05$).

Evaluations of MTF for different target-filter combinations

Figure 3 shows the combinations of all the MTF curves for the parallel and perpendicular orientations of the resolution test pattern. The MTF on the y-axis refers to the modulation value calculated from the sinusoidal intensity changes. The x-axis represents the frequency of the line pair of the resolution test pattern. The frequencies specified for the mammography procedure ranged from 5 lp/mm to 20 lp/mm.

Based on the parallel's curves, the overall score shows that the modulation gradually decreased with an increasing number of line pairs. The differences between 26 kV and 32 kV exposures in the 5–9 line pairs region were evident in both the test pattern orientations. The MTF value was calculated based on Bourne (5) and Table 1 shows

Table 1: MTF and MGD for different target-filter combinations for 26 kV and 32 kV

Target-filter	26 kV			32 kV		
	MTFa		MGDb (mGy)	MTFa		MGDb (mGy)
	Parallel	Perpendicular		Parallel	Perpendicular	
Mo-Mo	0.036	0.033	0.68 (0.001)	0.030	0.030	1.44 (0.0005)
Mo-Rh	0.042	0.061	0.57 (0.0009)	0.030	0.036	1.24 (0.0017)
Rh-Rh	0.043	0.038	0.75 (0.0005)	0.037	0.043	1.51 (0.0005)
One-way ANOVA						
F-statistics (df)	0.26(2,189)		49234 (2,12)	0.26 (2,189)		89972(2,12)
P value	> 0.05		< 0.05	> 0.05		< 0.05

[a]Mean MTF for frequency of 5 to 20 lp/mm.
[b]MGD (SD) between different target-filter combinations.
Abbreviations: MTF = modulation transfer function, MGD = mean glandular dose, SD = standard deviation, Mo = molybdenum, Rh = rhodium.

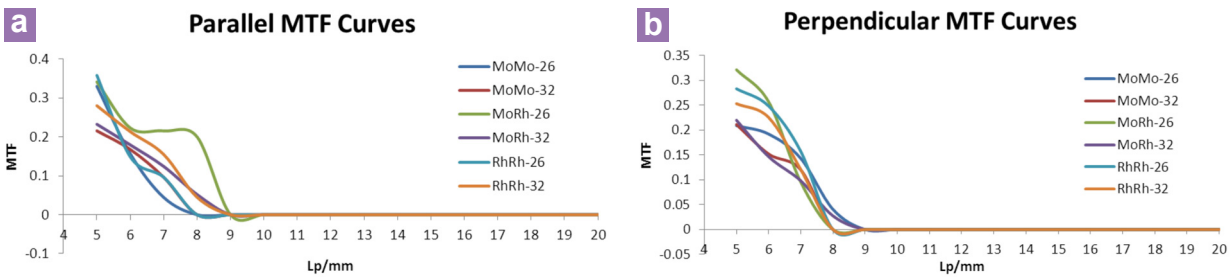

Figure 3: Modulation Transfer Function curves (a) for parallel and (b) for perpendicular oriented resolution test pattern as in Figure 1.

the mean MTF result. The one-way ANOVA for MTF evaluation shows that there is no significant difference between the target-filter combinations used with 26 kV and 32 kV images either in the parallel or perpendicular orientations to the chest wall side ($F(2,189) = 0.26$, $P > 0.05$).

Discussions

There is a significant difference among the average MGD values of Mo-Mo, Mo-Rh and Rh-Rh. Consequently, the result showed that all the MGD values were lower than the reference value specified by the National Radiological Protection Board (NRPB; 1999) in its DRL; MGD reference value for mammography was 2.0 mGy and the achievable MGD value was 1.5 mGy (15). The absorbed dose for glandular breast tissue was lower for 26 kV exposures than that for 32 kV exposure, implying that high-energy X-rays have more effective beam energy and higher penetration than low-energy X-rays (3).

The MGD varied according to the target-filter material used. The Mo-Rh combination yielded the lowest MGD values for both 26 kV and 32 kV exposures. The Rh-Rh combination generated the highest MGD values and the Mo-Mo combination produced the middle values. The combinations of the anode target elements with the filtration materials influence the spectrum of the X-ray energy. The Mo-Rh energy spectrum shows that it is capable of producing higher effective energy than Mo-Mo, even though both of them produce almost the same characteristic energy. This property makes Mo-Rh a more suitable choice for screening while using fixed tube voltage for normal breast thickness (16). Dance et al. (17), found that Mo-Rh dual anode tube produced an energy-broadened spectrum from the rhodium target with three characteristic peaks: at K_α energy, K_β (Rh) energy and a superimposed energy between K_α and K_β (Rh). This can be explained by the Rh target's design, which comprises a layer of rhodium deposited on a molybdenum backing. Therefore, some of the X-rays generated in the rhodium layer reached the molybdenum, producing a photoelectric effect. Consequently, Mo emitted its K-characteristic X-ray. This energy is lower than that produced by Mo and Rh K-edge, and it can be emitted from the target and inadvertently increase the MGD when filtered with Rh.

Table 1 demonstrates that as compared the standard Mo-Mo technique at 26 kV and 32 kV, the use of Mo-Rh target-filter combinations can yield better dose savings without the loss of spatial resolution. The results shows that all target-filter combinations gave only 8 to 9 lp/mm, which does not fulfil the minimum requirement by European Guidelines 2006 that the key performance for spatial resolution in digital mammography must exceed 12 lp/mm (14). Dance et al. (17), showed that in digital mammography, molybdenum anode could be optimally used for a breast thickness of 2–4 cm; however, the Rh-Rh target-filter combination was never selected. Their result also indicated that 26 kV was the optimal tube potential with Mo-Mo; however, Mo-Rh at 28 kV yielded the highest signal-to-noise ratio (SNR) for a breast thickness of 4–6 cm at an MGD of 0.6 mGy. An experimental study on the effect of X-ray beam hardening on detective quantum efficiency (DQE) and dose by Wong et al. (2), provides evidence that a reduction of 15% to 24% may be achieved by using Rhodium filters of 0.025 mm and 0.05 mm thickness without decreasing the image quality.

Our study results indicate that Mo-Rh yields a lower MGD value than Mo-Mo; this result is validated in Dance et al. (17). This proves that Mo-Rh is suitable for dose reduction in breasts with a thickness of 2–4 cm. Since Rh-Rh yields the highest MGD in the 4.5 cm breast phantom, Rh-Rh is more suitable for breasts thicker than 6 cm, because high-energy X-ray spectra from the Rh filter enables greater penetration, thereby providing a lower absorbed dose to the glandular tissues (17). According to Mehranian et al. (18), as the anode ages, the surface becomes rough, reducing the beam hardening effect and decreasing the absorbed dose; this decrease in absorbed dose is more significant in the case of lower tube voltage than higher tube voltage. This has raised the following question: should an aged tube (> 10 years) undergo a surface roughness investigation as a part of quality control for X-ray tubes? The MTF obtained using the resolution test pattern was also not as accurate as the LSF method, which uses a single slit pattern. Owing to these flaws, the computed radiography mammographic unit was no longer used clinically when this study was conducted. In future studies, the MTF should be computed using FT for the signal intensities as a part of the digital image quality assurance subroutine.

Conclusion

The choice of target-filter combinations and the tube voltages do not significantly influence the MGD values ($P < 0.05$). In reality, the combination of rhodium anode target and rhodium filtration

should retain the lowest MGD value compared to the other two target-filter combinations for a standard breast thickness (4.5 cm) with 50% glandularity. The actual intensity lost in X-ray spectra for lower tube voltage must be determined because anode roughness in aged tube was found to be one of the reasons that the actual result was different from the expected result. However, based on our MTF result, we can conclude that the resolution for different target-filter combinations does not significantly influence the MGD of 26 kV and 32 kV. Moreover, the orientation of the object while screening does not influence the resolution.

Acknowledgement

We would like to express our sincerest gratitude and thanks to the staff of the Medical Radiation Programme, School of Health Sciences and Department of Radiology, Hospital Universiti Sains Malaysia, for their support and help in this study.

Conflict of interest

None.

Funds

This work was supported by the Universiti Sains Malaysia Short Term Grant [304/PPSK/61311015].

Authors' Contributions

Conception and design, drafting of the article, critical revision of the article for important intellectual content and final approval of the article: SAAA
Collection, assembly, analysis and interpretation of the data: AKMS
Provision of study materials or patients, administrative, technical or logistic support: AZH

Correspondence

Ms Siti Aishah Abdul Aziz
MSc Medical Imaging Sciences (Curtin University of Technology)
Medical Radiation Programme
School of Health Sciences
Universiti Sains Malaysia Health Campus
16150 Kubang Kerian
Kelantan, Malaysia
Tel: +609-767 7623
Fax: +609-767 7515
Email: ishah@kb.usm.my

References

1. Hamed AR, Parinaz M, and Asghar M Evaluation of Mean Glandular Dose in a Full-Field Digital Mammography Unit in Tabriz, Iran. *Radiat Prot Dosimetry*. 2010. [cited 2010, Aug 4];**142(2–4)**:222–227. Available from: http://rpd.oxfordjournals.org/content/142/2-4/222.full.pdf+html?sid=8b352b3c-cec7-4aef-8e2b-624830747755.

2. Wong MD, Wu X, Li H. The effects of x-ray beam hardening on detective quantum efficiency and radiation dose. *J X-Ray Sci & Tech*. 2011 **19(4)**:509–519.

3. Bushberg JT, Seibert JA, Leidholdt Jr. EM, Boone JM. *The Essential Physics of Medical Imaging*. 2nd ed. Baltimore (US): Lippincott Williams & Wilkins 2002.

4. Ranger L, Samei. A technique optimization protocol and the potential for dose reduction in digital mammography. *Med Phys*. 2010;**37(3)**:962–969. doi: http://dx.doi.org/10.1118/1.3276732.

5. Bourne R. *Fundamentals of digital imaging in medicine*. London (UK): Springer-Verlag London Limited; 2010.

6. Desai N, Singh A, Valentino DJ. *Practical evaluation of image quality in computed radiographic (CR) imaging systems*. Canada (CA): Proceedings of SPIE Canada; 2010. p. 1–10.

7. Pre-owned Senographe DMR Mammography System [Internet]. United States (US): GE Healthcare; 2010 [cited 2012 Mar 26]. Available from: http://www.gehealthcare.com/usen/pre_owned_equipment/pre_owned_goldseal/products/mammodmr.html.

8. PTW-Freiburg. Diagnostic radiology products. Germany (DE): PTW; 2009. p. 19–20.

9. Mammographic Accreditation Phantom [Internet]. Norfolk (US): Computerized Imaging Reference Systems, Inc.; 2010 [cited 2012 Mar 08]. Available from: http://www.cirsinc.com/file/Products/015/015_DS_061510.pdf.

10. Gennaro G., Katz L., Souchay H., Alberelli C., and Maggio C., Are phantoms useful for predicting the potential of dose reduction in full-field digital mammography? Phys Med Biol. 2005; 50(8): p. 1851–1870. doi: http://dx.doi.org/10.1088/0031-9155/50/8/015.

11. Biomedical. Radiation Management Services Product Catalog 440.248.9300; Contrast and Resolution Mammography Phantom: Nuclear Associates Model 18-251-2000 (Optional Resolution Test Pattern, Model 07-555) [Internet]. United States (US): Fluke Biomedical; 2005 [cited 2012 January, 24]. Available from: http://www.srie.com.my/datasheets/FLUKE/Catalog/DI5.pdf.

12. (NIH). Image Processing and Analysis in Java (ImageJ) [Internet]. US: National Institute of Health, Federal Government US; 2004 [cited 2012 Jan 2]. Available from: http://rsbweb.nih.gov/ij/index.html.

13. Dance DR, Skinner CL, Young KC, Beckett JR, Kotre CJ. Additional factors for the estimation of mean glandular breast dose using the UK mammography dosimetry protocol. *Phys Med Biol*. 2000;**45(11):**3225–3240. doi: 10.1088/0031-9155/45/11/308.

14. Perry N, Broeders M, de Wolf C, Tornberg S, Holland R, Von Karsa L.European guidelines for quality assurance in breast cancer screening and diagnosis. Fourth edition: summary document. *Ann Onc*. 2008;**19(4)**:614–622. doi: 10.1093/annonc/mdm481.

15. International Commission on Radiological Protection (ICRP). Diagnostic reference levels in medical imaging: Review and additional advice. International: ICRP; 2001. p. 1–7.

16. Baldelli P, Phelan N, Egan G. Investigation of the effect of anode/filter materials on the dose and image quality of a digital mammography system based on an amorphous selenium flat panel detector. *Brit J Radiol*. 2010;**83(988)**:290–295. doi: 10.1259/bjr/60404532.

17. Dance DR, Thilander AK, Sandborg M, Skinner CL, Castellano IA, Carlsson GA. Influence of anode/filter material and tube potential on contrast, signal-to-noise ratio and average absorbed dose in mammography: A Monte Carlo study. *Brit J Radiol*. 2000;**73(874)**:1056–1067.

18. Mehranian A, Ay MR, Alam NR, Zaidi H. Quantifying the effect of anode surface roughness on diagnostic x-ray spectra using Monte Carlo simulation. *Med Phys*. 2010;**37(2)**:742–752. doi: http://dx.doi.org/10.1118/1.3284212.